Technical Note

Aspects of lead/acid battery technology 10. Cold-start performance

L. Prout
Aydon Road, Corbridge, Northumberland NE45 5EN (UK)

(Received March 10, 1993; accepted March 2, 1994)

Abstract

The factors that affect the performance of batteries when discharging at high rates and low temperatures are listed. The effect of changes in the mixing and pasting routines of allegedly identical batteries is discussed, together with the importance of the choice and amount of organic expander and the type/dimensions of the separators. The estimation of the component voltage losses is examined in detail with feasibility study to establish whether, or not, an existing battery design will meet a specified cold-start performance.

Introduction

The factors that affect the voltage performance of batteries when discharging at high rates at low temperatures are: (i) ohmic resistance of pillars and posts; (ii) ohmic resistance of connectors; (iii) ohmic resistance of the combined electrolyte paths; (iv) contact resistance between the grid and the active material; (v) the combined resistance of active material and grid; (vi) the resistance of separators; (vii) the polarization voltage at the active material, and (viii) the speed of diffusion of sulfate ions from the free electrolyte into the electrolyte that is absorbed by the active materials.

These factors can be subdivided into those for which a value of resistance can be calculated from dimensional data (or, at least, a close approximation derived using reasonable assumptions) and those for which the resistance cannot readily be calculated and which are much dependent on experimental data. Factors (i) to (vi) fall within the first category, whilst the remainder belong to the second category.

Pillars and connectors

The electrical resistance of the pillars and the connectors can be calculated from their relative dimensions. These resistances will change with change in temperature, as shown in Fig. 1.

Many battery performances are related to the temperatures of +25 and −18 °C. Over this range, both lead and antimony resistivities are reduced by approximately 20%. The effect of this is to lower the value of the voltage loss due to alloy resistance and, thereby, to improve the voltage performance of the cell on load.

SSDI 0378-7753(94)01924-K

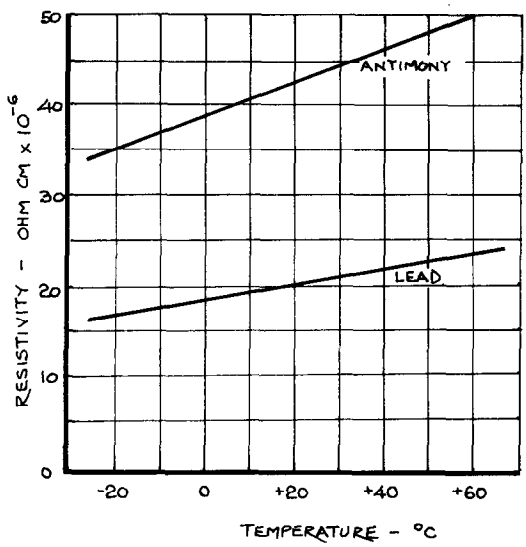

Fig. 1. Change of resistivity of lead and antimony with temperature.

Contact resistance between active material and grid

The coefficient of linear expansion of lead–antimony alloys is slightly less than that of pure lead. Thus, the shrinkage of pure-lead negative material is greater than the surrounding grid members. As a result, the pellets of negative active material will tend to loosen within the grid structure as the temperature decreases. This will cause the contact resistance between the material and the grid to increase and counteract the beneficial effect of the improvement in voltage loss in the pillars and connectors. The initial processing of the negative plates becomes vitally important in this context. Without correct control of paste mixing, flash drying and subsequent curing, the active material will not develop the interlacing network of needle-shaped crystals within the unformed and dried paste that: (i) confers to the material rigidity, good cementation and stability of dimensions, and (ii) enables the material to withstand satisfactorily the volume reduction that occurs in the formation process without a significant loss in apparent dimensions.

A number of operating factors can determine whether or not there will be a significant change in the external dimensions or sinkage/shrinkage of the individual pellets of material. The addition of an appreciable volume of water to the paste mixing to correct the paste density before application or the use of wet rollers after the plates have passed through the pasting hopper and before entry to the flash dryer are typical factors. In the former, additions of water after the main mixing do not blend homogeneously into the body of the paste. As a consequence, water is often squeezed out in the pasting process and is partly absorbed by the pasting belt with the remainder residing on the surface of the plates. Wet smoothing rollers produce the same effect of dripping wet plates as they enter the flash-drying oven. The oven temperature is increased to evaporate the surplus moisture and this tends to arrest

the curing process (or slow it down) with a subsequent loss of the self-supporting crystal structure that is necessary for a stable dimensioned plate.

To illustrate the pertinence of the above effects to battery performance, two allegedly identical paste mixings were used to make a particular battery with a nominal capacity of 40 Ah. In the first mix, the metering of the water and sulfuric acid was controlled accurately and no final water addition was needed to attain the designed paste density. In the subsequent pasting operation, the smoothing rollers were just moist enough to prevent plucking of the paste from the grid as the plate passed under the roller. Only occasional wipes with a damp sponge were needed to keep the rollers damp. In the second mixing, some of the initial water was withheld and, after mixing, considerable adjustment with water additions was needed to attain the designed paste density. During the pasting operation, the smoothing rollers were kept very wet so that the plates were dripping with water as they entered the flash-drying oven. The oven temperature had to be raised in order to dry off the plate surfaces before stacking for curing. Afterwards, both batches of plates were tank-formed and dry-charged. A comparison of their individual voltage performances at $3C_{20}$ A (i.e., 120 A) and $5C_{20}$ A (i.e., 200 A) at -18 °C is shown in Fig. 2.

Admittedly, it could be argued that these two conditions probably represent extreme conditions. Nevertheless, large voltage differences can arise in allegedly the same battery types and sizes as a result of an inadequately controlled paste-mixing procedure and poor pasting disciplines on the shop floor.

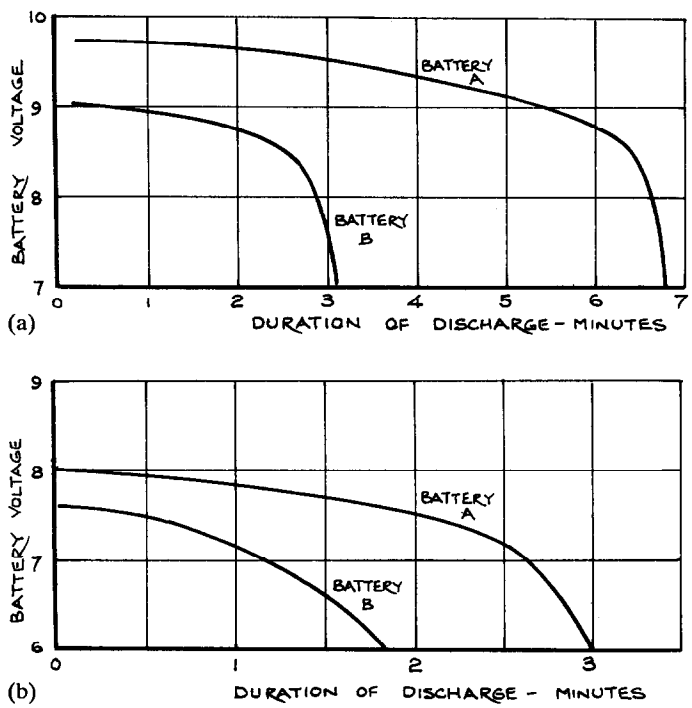

Fig. 2. Effect of changes in the mixing and pasting routines on the cold-start performance of allegedly identical 40-Ah batteries discharged at -18 °C; (a) discharge current $3C_{20}$ A (120 A), and (b) discharge current $5C_{20}$ A (200 A).

High-sulfation negative mixes produce a greater unformed solids volume and, in consequence, a greater volume reduction in the solid particles during formation. If, however, the flash-drying temperatures are just sufficient to evaporate the surface moisture without drying out the material in depth, these mixes exhibit a vigorous curing reaction. Furthermore, the latter reaction produces a relatively dense, interlacing network of needle-shaped lead sulfate crystals that resists shrinkage in the pellets when the solid particles decrease in size with formation.

High water mixes with low sulfation generally demand a somewhat higher flash-drying temperature and the risk exists of a degree of overdrying. The low sulfation level reduces greatly the proportions of tribasic and tetrabasic lead sulfates. As a result, there is less of the interlacing network of crystals produced and the crystal 'skeleton' is more susceptible to material shrinkage during formation. These mixes need greater care in processing, the formed surface tends to be more friable and presents a greater health hazard.

The addition of a barium sulfate expander can affect the shrinkage problem in negative materials. A greater amount of a relatively coarse barium sulfate is required to promote a rigid crystal structure than in the situation where the additive is fine. The particle-size distribution of the bought-in barium sulfate is worth examining on a routine basis. It is not sufficient to specify an amount of barium sulfate in a negative mix without qualifying the dominant particle size. Where facilities do not exist for the routine evaluation of the barium sulfate, the paste-mix specification should call for an excess over optimum to cater for possible variation in particle size. Although 0.3 wt.% of a finely divided barium sulfate is adequate for most mixes, it is not uncommon for the specification of the paste mixing to call for 0.5 to 0.6 wt.%. Certain reputable manufacturers of traction batteries have used as high as 3 wt.% of barium sulfate with considerable success.

For most applications, sulfuric acid (1.400 sp. gr.) addition of around 80 litres/tonne of oxide is generally acceptable. The water addition is adjusted to produce the required wet density.

No simple calculation of the losses due to the active material to grid contact resistance is possible due to the dependence of that factor on the excellence, or otherwise, of processing.

There are less difficulties with the positive plate. This is because the lead, lead oxide and lead sulfate in the cured but unformed plate are oxidized during formation and the process is accompanied by an increase in solids volume. Such a change has the effect of increasing the pressure of the active material on to the grid members and of improving the electrical conductivity at the material/grid interface.

Developed surface area of active material

With repeated high-rate discharges, there is a tendency for the negative active material to become passive and, thereby, give rise to a progressive loss of high-rate capacity. This has been attributed to a recrystallization phenomenon in the sponge lead of the charged negative. In addition to an additive to establish the highly porous structure, active anti-shrink agents are required to maintain that structure during the working life of the battery. These additives consist of organic expanders (such as humic acid and various forms of lignosulfonates) together with physical stabilizers (such as inert plastic fibres).

Lead sulfate and barium sulfate are isomorphic and have rhombic crystal lattices with very similar parameters. Highly dispersed barium sulfate introduced into the mass

of the negative active material provides numerous centres of crystallization for the lead sulfate that is formed on discharge and in the initial paste mixing. The result is for the lead sulfate to crystallize out on the barium sulfate crystals in preference to the metallic lead present. The initial porous structure is thereby set and the size reduction in the particles from lead sulfate to lead increases the volume of electrolyte in intimate contact with the material.

It is claimed that the particle size of the barium sulfate and the effectiveness of its even distribution throughout the negative paste mix sets the level of the true internal surface area of the active material, and with it the level of the true current density. Since the polarization voltage loss is a function of the true current density, the production of a highly developed internal surface area is essential for high cold-start voltages.

Sponge lead has a natural tendency to decrease its free energy. This tendency acts as a stimulus to recrystallization with a loss of developed internal surface area that increases the voltage polarization loss. The organic expanders are adsorbed at the surface of the lead metal. These compounds interpose adsorbed particles between the metal and the lead sulfate crystals and effectively prevent the formation of a dense layer of lead sulfate crystals on the metallic lead. As a result, access for electrolyte to the active material not yet converted to lead sulfate is maintained.

At low temperatures such as -18 °C, the high-rate capacity realizable is increasingly determined by the amount of electrolyte held within the pores of the active material. This is because diffusion inwards from the external free electrolyte is slow in comparison with the rate of formation of lead sulfate and the denuding of the electrolyte absorbed in the material of its sulfate content. The nature of the porous structure of the active material determines the magnitude of the polarization voltage loss. If the pores are of very small magnitude or diameter then, for a given porosity, there will be many more pores than if they had been of a larger diameter. For example, if there were ten times more pores in one material than in another of the same overall volume porosity, the internal surface area exposed to electrolyte could be forty to fifty times as great and the true current density reduced to some 2.5% of that with the larger pores.

The introduction of organic expanders assists the inorganic expander, barium sulfate, to preserve the highly developed structure, but not necessarily to create the initial structure. For this reason, good cold-start voltages stem from initially the use of a finely-divided, small particle-size oxide, typical of Shimadzu-type attrition mills or Barton pots, and the thorough incorporation of barium sulfate of comparable particle size evenly dispersed throughout the wet paste mix.

The choice of paste mixer and the standard of day-to-day maintenance has a big effect on the thoroughness of dispersion. It is advantageous to sample from a number of different locations within the bulk mix prior to discharging into the paste dispenser. For good reproducibility of voltage performance, the concentration of barium in any of the samples should not be less than 75% of the specified addition.

There are many different makes of organic expander, most of which are based on humic acid or metal lignosulfonates. The optimum amount of expander varies from one make to another and it is necessary to determine by experiment the best value to suit the lead oxide available and the mix formulation. With one make of purified organic expander, an oxylignin derived from sodium lignosulfonate, the makers recommend from 0.12 to 0.25% based on the weight of oxide. With less purified expanders, the quantities will be greater. The economics of manufacture often favour the use of the more purified material but this should be confirmed by practical testing.

In an earlier publication [1] on pastes and paste mixing it was shown that other substances, mainly organic dyes, have the same effect as humic acid and metal lignosulfonates. Some of these are considerably more effective than the lignosulfonates, but they tend to be expensive to an extent that they are economically unacceptable. The effect of a number of these organic dyes on pastes and paste mixing has been compared [1] with that of humic acid and sodium lignosulfonate. The results show that there is an optimum value for each expander for maximum effectiveness, e.g., the effect of adding 0.4 wt.% of sodium lignosulfonate was superior to adding 1 wt.%. This is common to most organic expanders and underlines the need to conduct careful experiments to derive that optimum for maximum performance at minimum cost.

Many of the organic expanders are water soluble and are best added as a water solution to the paste mixing, preferably during the initial water addition. In this way, the organic expander disperses rapidly and evenly throughout the mix. One proprietary brand of organic expander, Vanisperse A, produced by Borregaard in Norway, exhibits this characteristic of high water solubility in non-acidic conditions but, in the presence of the slightest acidity, gives very low solubility levels. The actual solubility is affected by the amount of expander per litre of solution. The following solubility figures are quoted by the supplier in Table 1.

The result of this low solubility is that during the water-addition stage of paste mixing, the organic expander disperses rapidly throughout the water/oxide slurry, but as soon as the sulfuric acid addition starts, it is thrown out of solution and remains as a fixed addition agent that is widely and evenly distributed between the lead oxides and lead sulfates. Unless the organic expander is fully dispersed before the sulfuric acid addition, the battery performances under cold-start conditions can be variable and unpredictable.

Electrolyte resistance

The electrolyte is present as free electrolyte between and around the plates, and as electrolyte absorbed within the active materials and the separation. The electrolyte within the active materials is a major contributor to the changes in both the voltage polarization losses and the resistance losses. These losses cannot easily be separated and measured. The best that can be done is to estimate the voltage losses in the free electrolyte and to include all other electrolyte losses in the voltage polarization losses.

The accepted method of estimating the separator resistance is to measure the combined resistance of the electrolyte path between plates with the separator interposed,

TABLE 1

Solubility of the organic expander, Vanisperse A, per litre of H_2SO_4 solutions to which varying amounts of the expander have been added

H_2SO_4 (sp. gr.)	Amount of expander added ($g\ l^{-1}$)	Solubility of expander ($mg\ l^{-1}$)
1.100	2.28	75
1.280	2.28	55
1.100	1.87	45
1.280	1.87	30

and then deduct the measured resistance of the electrolyte path without the separator. When estimating the resistance of the free electrolyte path in a cell element, the displacement of electrolyte by the separator is ignored and the dimensions of the path are taken as that of the free space between one plate surface and that of the facing surface of the adjacent plate.

The resistivity of dilute sulfuric acid increases with reduction in the temperature. For example, electrolyte of 1.280 sp. gr. has a resistivity at 25 °C of 1.25 Ω cm, but at −18 °C this rises to 3.2 Ω cm. Whereas a reduction in temperature causes a reduction in the voltage losses in the leady components, it gives rise to an increase in the losses in the electrolyte paths. These paths need to be kept as short as possible for good cold-start performance, i.e., the plates should be pitched as close together as the available separators, assembly techniques and the attainment of low-rate capacity will permit.

One approach is to use separators with a much reduced thickness. This, however, introduces the hazard of a very slack assembly with possible shedding of active material. Whilst this hazard can be overcome by placing packing shims on either side of each element, these reduce the available electrolyte in the cell and, hence, the possible low-rate capacity. Wherever a low-rate or reserve capacity is specified, the volumes of electrolyte available to positive and negative materials requires checking and, if necessary, the separator thickness must be adjusted to ensure that sufficient electrolyte is available to sustain that required capacity.

The use of packing shims introduces an extra operation and an extra component cost. It is more economic to dispense with shims and to adjust the thickness of the back web of the separator.

In any cell, there will be two electrolyte paths in parallel per pitch. The length of each path will be the distance between adjacent facing plates. The cross-sectional area of the path will be the single surface area of a plate. If, in a cell rated at 40 Ah (20-h rate), there are 4 positive and 3 negative plates with single surface areas of 100 cm^2 and spaced at 0.25 cm apart, then:

effective length of a single path = 0.25 cm

effective cross-sectional area = 100 cm^2

number of paths in parallel per cell = 2 × number of positive plates = 8

If the cold-start current requirement is $4.5C_{20}$ (equivalent to 180 A) and the resistivities of a sulfuric acid solution of 1.280 sp. gr. are 1.25 Ω and 3.2 Ω cm, at 25 and −18 °C, respectively, then:

resistance of a single electrolyte path at 25 °C = 1.25 × 0.25/100 = 0.0031 Ω

resistance of a single electrolyte path at −18 °C = 3.2 × 0.25/100 = 0.008 Ω

voltage loss per cell at 25 °C = 0.0031 × (180/8) = 0.070 V

voltage loss per cell at −18 °C = 0.008 × (180/8) = 0.180 V

The reduction in temperature from 25 to −18 °C has caused the battery voltage loss in the electrolyte in a 6-cell unit to increase from 0.42 to 1.08 V, or an increased loss of 0.66 V.

Many specifications ask for a minimum of 8.4 V for a 6-cell battery at the end of the cold-start test discharge. At −18 °C, the total loss of 1.08 V represents almost a quarter of the total permissible loss. This is a big proportion of the total and highlights the importance of proper consideration being given to plate pitch or, if the

pitch is fixed, to looking for every opportunity in other areas of reducing voltage losses.

It is insufficient in a design just to fill the cell compartment comfortably using readily available plates. The design aim should be to achieve the minimum spacing between plates that will give the low-rate or reserve capacity, and to seek other means to maintain a light pressure on the element within the compartment even though this has to be low displacement spacers and an extra cost item.

As the discharge proceeds, the electrolyte concentration falls. The resistivity curves over the range 1.280 to 1.190 sp. gr., i.e., where the minimum resistivity occurs, are relatively flat so that the proportion of voltage loss ascribed to the electrolyte path does not alter materially over the cold-start discharge.

Separators

The separator is often overlooked as a significant factor in determining the voltage loss in a cell during a cold-start discharge. There is a tendency for the separator to be chosen on the basis of lowest price or availability, with the voltage performance of secondary importance. This can only be tolerated where the cold-start voltage and duration is readily obtained without recourse to any carefully chosen design or component. This rarely happens and the incidence of its occurrence has become even rarer with the introduction of smaller diameter starter motors and the specification for lower reserve capacities. These have caused the specified minimum voltages for satisfactory starting under adverse conditions to be increased so that the regular attainment of reliable starting has become more and more difficult. Not only has the low-rate battery capacity been reduced, but the minimum voltage for cold starting has been raised, e.g., for a 12-V battery at -18 °C, some car makers require a minimum voltage of 9 V after 1 min discharge at $5C_{20}$ A and -18 °C. With requirements such as these, a very close look at the separator used becomes vital.

Allegedly similar separators sold in competition with each other exhibit large differences in electrical resistance at these high discharge rates. Small differences in physical make-up can often confer on the revised separator appreciable improvements in resistance and the voltage loss apportioned to them. For example, it is known that a slackly assembled element will give a better cold-start voltage than a tight assembly. Corrugated separators provide a reservoir of electrolyte adjacent to the negative material and this assists the negative performance. Intentional bowing of the back web of the separator will do much the same. Fine ribbing on the back of the separator spaces the separator away from the negative material and achieves a similar result.

Intentional slack assemblies are not a reliable design approach since mechanical trouble occurs under severe vibration and the lack of restraint on both active materials leads to: (i) excessive expansion, particularly of the negative, and (ii) increased risk of premature failure on life due to self-discharge paths being created fortuitously within the cells by dislodged material from the loosened surfaces of the plates. Differences in the degree of slackness are reflected in variable cold-start performances so that the interplay of permitted tolerances in such situations deny the design any predictability.

The data shown in Figs. 3 and 4 illustrate the effect of separator change on the voltage performances of 12-V, 45-Ah (20-h rate) batteries with the same plates and element construction and required to meet the same performance specification. The three separators (termed A, B and C) were all deemed to be similar and suitable for the battery in question. The plates used in the comparison were all taken from the

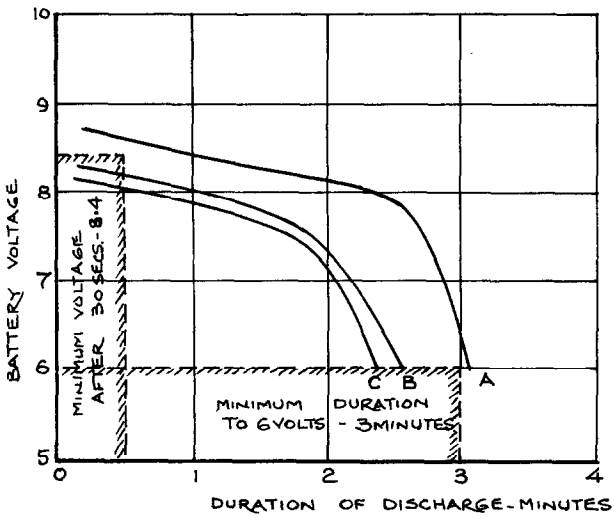

Fig. 3. Effect of allegedly similar separators on the cold-start voltage performance of a battery 12-V, 45-Ah discharging at 220 A at −18 °C.

Separator	*Resistance at 25 °C (Ω)*	*Resistance at −18 °C (Ω)*
A	8.15×10^{-3}	11.5×10^{-3}
B	9.0×10^{-3}	13.0×10^{-3}
C	8.6×10^{-3}	13.2×10^{-3}

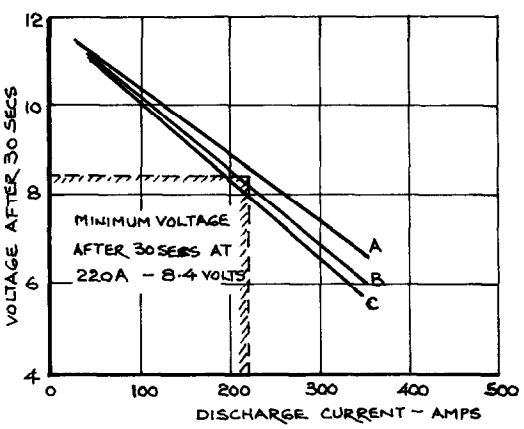

Fig. 4. Effect of allegedly similar separators on the variation of voltage after 30-s discharge at −18 °C of a 12-V, 45-Ah battery with differing discharge currents.

Separator	*Resistance at 25 °C (Ω)*	*Resistance at −18 °C (Ω)*
A	8.15×10^{-3}	11.5×10^{-3}
B	9.0×10^{-3}	13.0×10^{-3}
C	8.6×10^{-3}	13.2×10^{-3}

same production batch and selected for close weight agreement. The separators were all made from resin-impregnated paper to the same overall thickness.

The make-up of the cells were 5 positive and 6 negative plates interleaved with 10 separators. In the calculation of the voltage losses due to the resistance of the separators in a cell element, all the separators are in parallel and thus make the effective resistance of the 10 separators in the element one-tenth of the resistance of one separator i.e., in the case of separator A, the effective resistance per cell would be 0.00115 Ω.

Based on a cold-start current of 220 A (i.e., $4.9C_{20}$ A) at −18 °C, the calculated voltage loss per cell due to separator resistance will be:

$$\text{voltage loss} = \frac{\text{separator resistance} \times \text{cold-start current}}{\text{number of separators per element}}$$

The voltage losses per 12-V battery at 220 A and −18 °C, calculated as above, for each separator are given in Table 2. When the calculated results are compared with the differences between the voltages after a 30-s discharge shown in Fig. 3, there is an apparent discrepancy of between 0.2 and 0.3 V, the differences shown on the curves are the greater. This discrepancy can be explained by the possible differences in the actual electrolyte concentrations in the active materials due to variable diffusion characteristics of the separators, the absence or otherwise of some free electrolyte in contact with the surface of the negative material or, perhaps, uneven distribution of the impregnating resin in the separators.

Irrespective of the reason(s), there is some justification to increase the value of the voltage loss derived from a calculation based on the measured resistance of the separator. A difficulty exists in deciding how much that increase should be, but over many measurements a prudent increase seems to be between 10 and 12%. In examples which follow, a factor of 10% is taken in estimations of the voltage loss due to separators for want of a better and more reliable factor based on widespread data.

In the example quoted, the application of the reconciliation factor would make the probable voltage losses due to separators A, B and C increase to the values given in Table 3. These voltage losses are large and, compared with the permissible maximum voltage loss from 12.8 V on open circuit to 8.4 V will represent close on 40% of that allowance. The choice of separator becomes one of the important factors in the design of a battery for cold-weather starting.

The influence of the thickness of the back web of a separator in determining the magnitude of the voltage loss due to the separator should not be underestimated. For example, in a sintered polyethylene separator, the reduction in the back-web thickness from 0.5 to 0.25 mm brought about a reduction in resistance from 0.23 to 0.12 Ω

TABLE 2

Voltage loss due to separator resistance

Separator	Voltage loss		Increased volt loss compared with separator A at −18 °C
	−18 °C	25 °C	
A	1.52	1.06	
B	1.72	1.19	0.20
C	1.74	1.14	0.24

TABLE 3

Voltage loss due to separator resistance

Separator	Voltage loss at −18 °C	Voltage loss at 25 °C
A	1.67	1.17
B	1.89	1.31
C	1.91	1.25

cm^{-2}, i.e., about 50% reduction. If this is applied to separator A, a voltage improvement of about 0.6 V would accrue. It is tempting to ask where could a voltage saving of this order be more easily obtained. Certainly not in the area of the metallic components without greatly increasing the material costs.

In the light of these data, it is not surprising that some manufacturers have moved over to the use of thin sintered plastic separators with what appears to be disproportionately thick ribs. The control of the thickness of the back web to as low as 0.25 mm is not difficult and the reproducibility is good in bulk production.

An essential to any cold-start designing is the knowledge of how separator resistance will change with a change in temperature and the extent to which proprietary makes of separator vary one from the other.

Influence of grid design

This is a particularly difficult area to evaluate since both the active materials and the grid members conduct current and both are in direct contact with each other. In effect, the two conducting media are in parallel with each other, apart from the factor of the contact resistance between the active material and the grid members.

The main current paths are from top to bottom when charging and from bottom to top when discharging, distorted to some extent by the grid to active material conductivities. The latter tends to change during a full discharge due to the production of poorly conducting lead sulfate in those areas where there is the greatest conductivity between active material and grid, i.e., at the contact points between grid and material. At high discharge rates, the amount of lead sulfate produced is not so great that the changing distribution of this compound alters markedly the broad generalized current distribution of the fully-charged plate.

This leads to an empirical assessment of the voltage losses in a well-cured plate, based on an assumption that the equivalent circuit consists of two conducting paths in parallel. The first path comprises the effective conductivity of all the vertical members of the grid, i.e., the sum of all the vertical ribs and the side-frame members. The second path, in parallel with the first, is a composite of the active material and the horizontal wires or pins. The horizontal wires can be looked upon as high conductivity reinforcing bars in the active material.

The following empirical rules can be applied in order to arrive at a reasonable estimate of the resistance of each of these paths:

(i) *Grid-member path.* Take the sum of the cross-sectional areas of all ribs and the two side frames as the cumulative cross-sectional area of this path, and the length of a rib plus the width of the top frame as the effective length of the path. Using

the appropriate value of resistivity, as determined by the metal contents of the alloy and the temperature, the resistance R_g of this path can be calculated.

(ii) *Active-material path*. Convert the total horizontal grid metal into equivalent active material by multiplying the volume of metal in the wires by the ratio of resistivity of active material to resistivity of grid alloy. Add this equivalent volume of wire material to the volume of active material and divide the result by the same length figure as used for the grid-member path. This gives an equivalent cross-sectional area for the active material and the horizontal grid metal. Using the appropriate resistivity value for the active material in a porous form, derive the resistance of the active material path R_m.

The equivalent plate resistance R_p is then calculated from the relationship:

$$1/R_p = 1/R_g + 1/R_m \quad (1)$$

The voltage loss will then be the product of the average plate current and the resistance R_p. As the current is increasing from zero at the bottom of the plate to the full discharge current at the top frame, the average current can be taken as half the full-plate current, i.e., half the cell discharge current divided by the number of plate pitches in a cell.

In negative plates the active material is a pure-lead sponge with good particle-to-particle contact. The resistivity of pure porous lead is given by Crennell and Lea [2] as 18.3×10^{-5} Ω cm, whilst that of porous lead dioxide is stated by Thomas [3] as being 74×10^{-4} Ω cm at 25 °C. At −18 °C, these would be about 14.8×10^{-5} and 60×10^{-4} Ω cm, respectively.

The resistivity of a Pb–6wt.%Sb alloy at −18 °C is about 2×10^{-5} Ω cm. The large disparity between the resistivity of lead or antimonial lead alloy and lead dioxide emphasizes the importance of low-resistance vertical ribs in a positive grid more so than in a negative grid. During the working life of a battery, the rib and wire material in a positive grid oxidizes to lead dioxide and the conductivity of the grid members decreases. Practically all the wire material and an appreciable proportion of the rib material is converted to lead dioxide and this results in an increase in the voltage losses in the positive plate as the battery ages.

To limit capital investment in grid moulds and to reduce the investment capital in grid stocks, a common grid is sometimes adopted for both positive and negative plates. In this case, the dimensions of the grid members have to be thicker (to accommodate oxidation of the positive) than would be necessary for a matching negative. Since this rationalization exacts a cost penalty, the economics of the principle of common grids should be carefully assessed before adopting it as a design policy. It is rarely worthwhile, except in the case of special low-demand types, and the need to manufacture these types should be carefully examined.

Plate voltage polarization

This is directly related to the magnitude of the internal wetted surface area of the active material. This phraseology is used since the volume porosity of several active materials can be substantially equal but their internal surface areas can differ considerably dependent on the mean pore diameters. Much depends on: (i) the distribution of the barium sulfate and how effectively it is dispersed throughout the active material; (ii) the efficiency of the organic expander in preventing the formation of a film of poorly conducting lead sulfate over the surface of the active material, and (iii) the reduction of the exposed surface area of the material.

It is not possible to quantify these conditions, even by simple empirical rules. For convenience, all losses other than those that can be estimated from dimensional data are often loosely grouped under the generic term of 'polarization losses'. Using this approximation the voltage polarization losses would become the difference between the total voltage loss on load and the sum of the voltage losses in pillars, connectors, free electrolyte, separators and grid/active materials. Technically, this is open to considerable academic criticism. The object of all designing is, however, to arrive at a workable answer that closely represents reality even though the method employed may not be wholly substantiated by theory.

It is enlightening to work through a typical commercial battery design to isolate the individual voltage loss, and to calculate and compare those losses. The order of voltage loss will reveal the major problem areas and, therefore, where design and/or experimental work should be concentrated if the resulting voltage under cold-starting conditions fails to be acceptable and the original design requires improving. This is illustrated in the following exercise using a battery that is typical of one of a maker's current range.

Estimation of component losses in a typical battery

Consider a battery of 6 cells rated at 45 Ah capacity (C_{20} rate) and comprising 5 positive and 6 negative plates interleaved with 10 resin-impregnated separators. The specified cold-start requirement is a minimum duration when discharging at 220 A at −18 °C for 3 min to 6 V with a minimum voltage of 8.4 V after 30 s of discharge. The following physical data apply:

grid dimensions (mm)	144 (width) × 100 (height) × 1.6 (thickness)
lug dimensions (mm)	16 (width) × 6 (height) × 1.6 (thickness)
side frames (average) (mm)	2.5 (width) × 1.6 (height) × 100 (length)
top and bottom frames (mm)	2.5 (width) × 1.6 (height) × 139 (length)
number of vertical ribs	7
rib dimensions (mm)	1.3 (width) × 1.6 (height) × 95 (length)
number of horizontal wires or pins	20
dimension of one row of wires ($cm^2 \times mm$)	0.005×129
apparent volume of negative material (cm^3)	17.2
apparent density of negative material ($g\ cm^{-3}$)	3.6
apparent volume of positive material overpasted by 0.1 mm (cm^3)	18.3
apparent density of positive material ($g\ cm^{-3}$)	3.7
dimensions of separator (mm)	148 (width) × 108 (height) × 1.4 (thickness)
thickness of back web (mm)	0.5
plate pitch (mm)	6.6
equivalent dimensions of intercell connection ($cm^2 \times cm$)	0.7×10.1
equivalent dimensions of end pillars ($cm^2 \times cm$)	0.5×4.8
resistivity of pure lead at −18 °C (Ω cm)	1.65×10^{-5}
resistivity of Pb–6wt.%Sb alloy at −18 °C (Ω cm)	2×10^{-5}
resistivity of porous lead dioxide at −18 °C (Ω cm)	60×10^{-4}

resistivity of 1.28 sp. gr. electrolyte at −18 °C (Ω cm)	3.2
d.c. resistance of separators at −18 °C (Ω)	9.0×10^{-3}

(i) Voltage loss in pillars

length (cm)	4.8
cross section (cm²)	0.5
resistance (Ω)	$2\times10^{-5}\times4.8/0.5=19\times10^{-5}$

Since there are two pillars per battery, the resistance of the pillars per battery will be 38×10^{-5} Ω.

(ii) Voltage loss in connectors

length (cm)	10.1
cross section (cm²)	0.70
resistance (Ω)	$2\times10^{-5}\times(10.1/0.7)=28.9\times10^{-5}$

Since there are 5 connectors per battery, the resistance of the connectors per battery will be 144.5×10^{-5} Ω.

Overall, the voltage loss at 220 A in pillars and connectors will be: $220(38.4+144.5)\times10^{-5}=0.41$ V.

(iii) Voltage loss in free electrolyte. The average distance between positive and negative plates will be half the difference between the plate pitch and the sum of the positive and negative plate thicknesses, i.e., 0.5 (6.6 − 1.6 − 1.7) = 1.65 mm. This will be the effective length of the electrolyte path.

single plate surface area (cm²)	$13.9\times9.5=132.1$
effective surface area of 10 separators (cm²)	1321
resistance of free electrolyte path (Ω)	$3.2\times(0.165/1321)=0.0004$
total resistance of electrolyte for 6 cells (Ω)	0.0024
voltage loss in electrolyte per battery (V)	$220\times0.0024=0.528$

(iv) Voltage loss in separators

resistance of one separator (Ω)	9×10^{-3}
resistance of 10 separators in parallel (Ω)	0.9×10^{-3}
voltage loss per battery with a reconciliation factor of 1.1 (V)	$220\times1.1\times6\times0.9\times10^{-3}=1.31$

(v) Voltage loss due to grid and active-material resistance

• For the negative plate:

apparent volume of active material (cm³)	17.2
apparent density of active material (g cm^{-3})	3.6
true density of active material (g cm^{-3})	11.3
true volume of active material (cm³)	$17.2\times(3.6/11.3)=5.5$
volume of metal in grid wires (cm³)	$20\times0.005\times12.9=1.3$
active material equivalent of wire volume (cm³)	$1.3\times(14.8\times10^{-5}/2\times10^{-5})=9.62$
equivalent volume of wire metal and active material, expressed as active material (cm³)	$5.5+9.62=15.12$
equivalent cross-sectional area of wire metal and active material (cm²)	$15.12/9.5=1.59$
cumulative resistance of wires and active material (Ω)	$14.8\times10^{-5}\times(9.5/1.59)=88.4\times10^{-5}$
equivalent cross-sectional area of ribs and side frames (cm²)	$7(0.13\times0.16)+(2\times0.25\times0.16)\approx0.23$
length of ribs and side frames (cm)	13.9
cumulative resistance of ribs and side frames	$2\times10^{-5}\times(13.9/0.23)=120.9\times10^{-5}$
effective resistance of wires and active material and ribs and side frames in parallel (Ω)	51.0×10^{-5}

resistance of plate lug (Ω)	$2\times10^{-5}\times(0.6/1.6\times0.16)=4.7\times10^{-5}$
effective plate resistance (Ω)	$(51.0+4.7)\times10^{-5}=55.7\times10^{-5}$
voltage loss per cell due to the resistance of negative plate (V)	$0.5\times(220/5)\times55.7\times10^{-5}=0.0122$
voltage loss per battery due to negative plates (V)	$6\times0.0122=0.074$
• For positive plate:	
apparent volume of positive material (cm^3)	18.3
apparent density of positive material (g cm^{-3})	3.7
true density of positive material (g cm^{-3})	9.4
true volume of positive material (cm^3)	$18.3\times(3.7/9.4)=7.2$
volume of metal in grid wires (cm^2)	1.3
active material equivalent of wire volume (cm^3)	$1.3\times(60\times10^{-4}/2\times10^{-5})=390$
equivalent volume of wire metal and active material expressed as active material (cm^3)	$7.2+390=397.2$
equivalent cross-sectional area of wire metal and active material (cm^2)	$397.2/9.5=41.8$
cumulative resistance of wires and active material (Ω)	$60\times10^{-4}\times(9.5/41.8)=136.4\times10^{-5}$
cumulative resistance of ribs and side frames (Ω)	120.9×10^{-5}
effective resistance of wires and active material and ribs and side frames in parallel (Ω)	64.1×10^{-5}
resistance of plate lug (Ω)	4.7×10^{-5}
effective plate resistance (Ω)	$(64.1+4.7)\times10^{-5}=68.8\times10^{-5}$
voltage loss per cell due to the resistance of the positive plate (V)	$0.5\times(220/5)\times68.8\times10^{-5}=0.015$
voltage loss per battery due to the positive plates (V)	0.09

Thus, when discharging at 220 A at -18 °C, the total voltage loss per battery due to the positive and negative plates is estimated to be $(0.09+0.074)=0.164$ V.

(*vi*) *Polarization losses*. For the purpose of this example, it is assumed that the average voltage of a number of the chosen batteries discharging at 220 A and -18 °C was 8.38 V after 30 s. The open-circuit voltages at -18 and 25 °C were 12.4 and 12.7 V, respectively. These values are representative of real batteries made with common grid castings for positive and negative plates; any findings from the estimations represent actual conditions and not 'made-up' conditions. On average, the voltage loss after 30 s discharge at 220 A and -18 °C would be 4.02 V. Previously, it was stated that, for convenience, the voltage polarization loss nomenclature would be given to all those voltage-loss areas where a value for the loss could not be quantified by simple empirical rules or by consideration of dimensional data. Using this loose terminology: voltage polarization loss = voltage loss on load minus sum of voltage losses in pillars, connectors, electrolyte, separators and plates. This would give a voltage loss of 1.61 V for this area.

In order of magnitude, the individual voltage losses can be allocated as follows:

voltage polarization (V)	1.61	(40%)
separator resistance (V)	1.31	(33%)
free electrolyte (V)	0.53	(13%)
pillars and connectors (V)	0.41	(10%)
grid and active material (V)	0.16	(4%)

The actual values of the individual losses will vary to some extent with the particular design but, in general, the order of importance of the voltage-loss generating areas will remain substantially the same.

In seeking to improve a poor cold-start voltage, it is of little value to make changes in the pillar and connector designs if the size of the voltage improvement sought

approaches, is equal to, or exceeds the calculated loss in the pillars and connectors. A disciplined approach is needed and should concentrate on minimizing the effect in each of the main loss-making areas and reducing the losses in the others. In the preparation of any redesign, it is helpful to undertake the following actions.

(i) Comparison of the resistance of as many makes and types of separator as possible at normal and low temperatures relevant to the purchaser's specifications. Selection of those that are clearly better than the average and rejection of those that are marginally acceptable, but have a back face that is virtually flat in contact with the negative plate. If, subsequently, it is found that the cold-start voltage is readily achieved, then accept the most economic separator of those found suitable.

(ii) Selection of either a ball-mill oxide of fine particle size or an equivalent Barton-pot oxide with an acid absorption value of the order of 20 cm^3 of H_2SO_4 per 100 g of oxide. Processing of the oxide to the minimum formed density that will not develop sinkage or shrinkage in the pellets away from the grid members. It is particularly useful to have available a small paste mixer of about 15 kg capacity in which to try out mixings, even though the plates may have to be hand-pasted for the trials. If the paste can operate satisfactorily with this handling, it is fairly certain that it will work in a large mixing and is amenable to machine pasting.

(iii) Determine the optimum addition of organic expander for maximum cold-start voltage and maintenance of cold-start duration at the relevant low temperature. Here, the availability of a small mixer is invaluable. In general, it is better to concentrate on using the purest forms of proprietary organic expanders even though at first sight they may appear to be more expensive than others that are offered.

(iv) Evaluation of the particle-size distribution of the barium sulfate. This should be similar to that of the lead oxide. If it is coarser, then change over to the addition of the barium sulfate expander as 'barium milk', i.e., convert barium hydrate to the sulfate in a liquid form as described in ref. 1.

(v) Pitch the plates as close as the assembly facilities permit and take up any excess space with corrugated or porous side packings to minimize the extra displacement of electrolyte.

(vi) Pay particular attention to the curing of the plates to achieve a good interlacing crystal structure that is essential for a strong pellet structure capable of supporting itself in service use. This will minimize the active material to grid contact resistance.

(vii) Adopt the shortest connector path between cells and avoid multiple fusions, i.e., reduce the number of components that have to be fused to each other to as low as the manufacturing equipment will permit. In this respect, the adoption of 'upside-down' casting of integral straps, connectors and pillars to an assembly of plates offers a considerable easement to production and a reduction in the variability of fused joints and their conductivity problems.

(viii) Allocate as much metal to the vertical ribs of the grid as possible without affecting adversely either the retention of the pellets of active material within the grid or the rigidity of the grid.

(ix) Obtain competitors' equivalent batteries that are known to have met the cold-start requirements and derive comparative performance data and component voltage-loss figures. From this data, it is possible to pinpoint where the greatest differences occur and where to concentrate design and processing efforts. If the loosely defined voltage polarization losses differ significantly from one's own figures, then attention should be centred on the activity of the oxide selected or the amount of organic expander that has been used.

Irrespective whether one's own product can meet a cold-start requirement or not, the exercise with competitors' products will indicate in advance where the greatest effort in design and/or processing should be directed to meet future challenges before they become financially damaging. Changes in design and processing take time to put into bulk production and, in that time, a manufacturer's share of the market can be eroded.

So often there is neither the time nor the resources immediately available to provide, by careful experimentation, the information that will define the optimum expander levels, the least resistive separator, or the best type of oxide. Nevertheless, a decision whether or not a realistic design, not necessarily the best, can or cannot be produced using existing production facilities has to be made and, usually, enacted quickly. In these circumstances, an estimation has to be made using data that relate to current products in order to determine the feasibility, or otherwise, of coming close to, or meeting, the new requirement.

Feasibility of meeting a specified cold-start performance based on an existing design of battery already in current production

Consider the existing battery to be one with cells that contain 9 plates, rated at 12 V and 40 Ah (C_{20} rate), and assembled in a thin walled polypropylene monobloc container that measures: 236 mm (L) × 135 mm (W) × 205 mm (H). High-rate discharge data exist, at 25 and −18 °C, on both the voltages after 30-s discharge and the durations of discharge to an end voltage of 6 V. These data are common in the industry to define the engine-starting capability of a battery. This information for the selected battery is plotted in Figs. 5 and 6. The new design requirement is for a battery that uses the same thin walled container but has a cold-start performance that gives a minimum voltage of 9.0 V after 30 s at 210 A and −18 °C and a minimum duration to 6 V of 3 min.

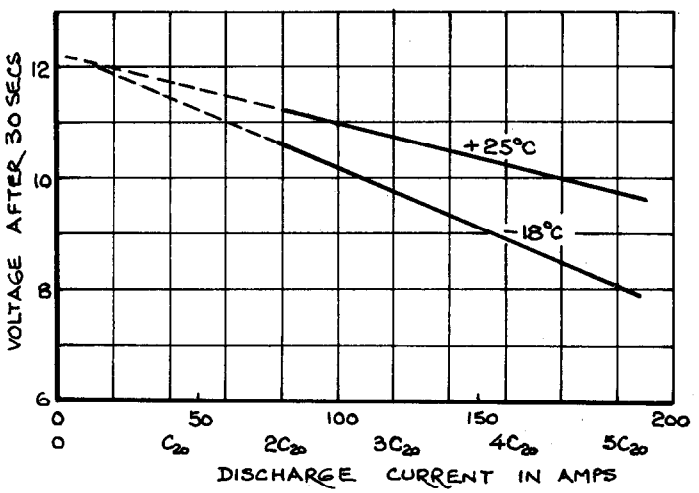

Fig. 5. Average voltage after 30-s discharge at 25 °C and −18 °C for different discharge currents; see text for battery specification.

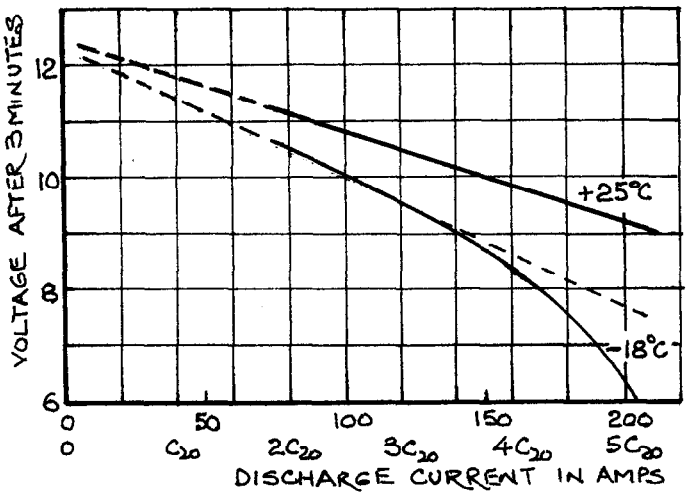

Fig. 6. Average voltage after 3-min discharge at 25 and −18 °C for different discharge currents; see text for battery specifications.

The data indicate the following two features:

(i) At 25 and −18 °C, the average voltage loss at 30 s is proportional to the discharge rate up to and including $5C_{20}$ A (i.e., 200 A). There is ample absorbed electrolyte to maintain a level of voltage polarization that is proportional to the discharge current up to $5C_{20}$ A.

(ii) There is a divergence from linearity at −18 °C after 3 min as the current approaches $3.5C_{20}$ A (i.e., 140 A). The divergence increases in rate as the current increases. This indicates that the volume of absorbed electrolyte should be increased to limit the fall in concentration within the pores of the active material as the discharge proceeds. Such a modification would extend the duration of the linear portion of the voltage–current curve.

Before starting to make design changes, it is important to examine the limits of variation from the average data. This is because there will be variations in production and unless the design caters for these, there is a risk of underestimating the change that is needed. Figure 7 shows data for the range of variations in the voltage after 30-s discharge at 25 and −18 °C. Figure 8 gives similar data for voltages after 3 min. Whilst there is linearity between the maximum and minimum voltages after 30-s discharge up to $5C_{20}$ A (i.e., 200 A), divergence from a linear relationship does occur after a 3-min discharge as the performance at −18 °C approaches the minimum. The following observations are made:

(i) The existing design would not approach the minimum voltage requirement of 9 V after 30 s at −18 °C when discharging at 210 A, even though the original low capacity rating of 40 Ah might have been generous and frequently exceeded in bulk production.

(ii) Plotting the voltages after 3 min at −18 °C on probability paper (on the basis that the voltages shown on the curves do not represent the absolute maximum and minimum limits but are probably nearer the 2-σ limits) shows that there is a probability that about 15% of the bulk production would not reach the minimum voltage of 6 V. This might not be serious in actual service since the proportion of cases where the limiting conditions of 3-min discharge occur would not be high.

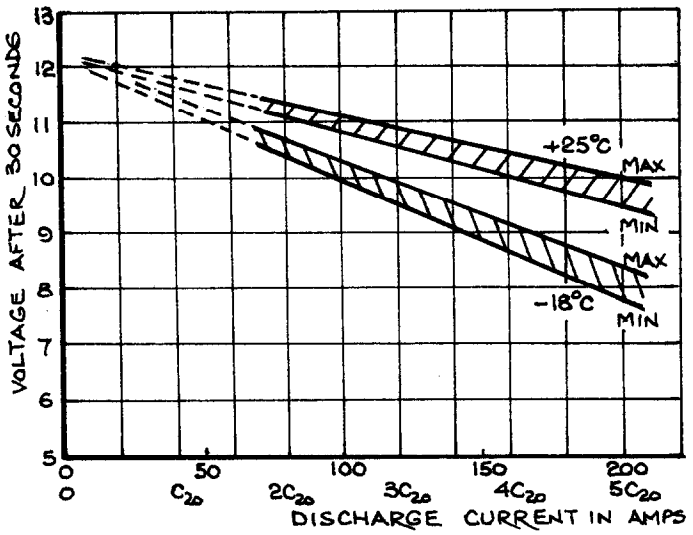

Fig. 7. Envelope of maximum and minimum voltages after 30-s discharge for varying current at 25 and −18 °C.

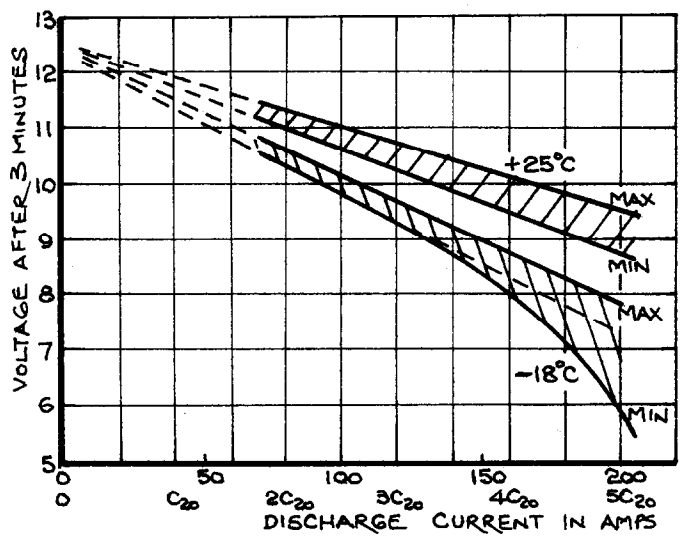

Fig. 8. Envelope of maximum and minimum voltages after 3-min discharge for varying current at 25 and −18 °C.

(iii) Attainment of the minimum voltage after 30-s discharge is the controlling design requirement and some deviation from the type and thickness of plate and, possibly, some change in the pillar/connector will be necessary.

Whilst the convention of referring to the cold-start current as a multiple of the low-rate capacity is helpful when compiling standard specifications, so much depends on how generous is the design in providing that low-rate capacity. Depending on the

differences that exist between the actual and rated capacities, the performance characteristics at high rates and low temperatures can appear better or worse than equivalent batteries, although the actual differences between the cold-start capacities and the voltage performances may be small. In specific designs, it is the actual performance that matters.

As long as the mixing procedures and formulations are constant for a range of batteries, so will be the nature of the porous structure created in the active materials. The voltage performance of this structure will be a function either of the apparent surface area for a constant discharge current, or of the apparent current density where the discharge current differs from the standard battery. For ease of comparison, it is convenient to divide the total current per cell by the product of the number of positive plates and the single surface area of a positive plate. This current is termed the 'apparent current density.' The pattern of the change in plate voltage will follow the curve of voltage versus apparent current density as long as: (i) the pillars and connectors are unchanged; (ii) the free electrolyte path dimensions are unchanged; (iii) the same separator back web is used, and (iv) the plate thicknesses are not increased. Such a curve will set the maximum apparent current density for the projected new design. The average performance data at −18 °C for the standard 12-V, 40-Ah battery has been replotted on this basis in Fig. 9.

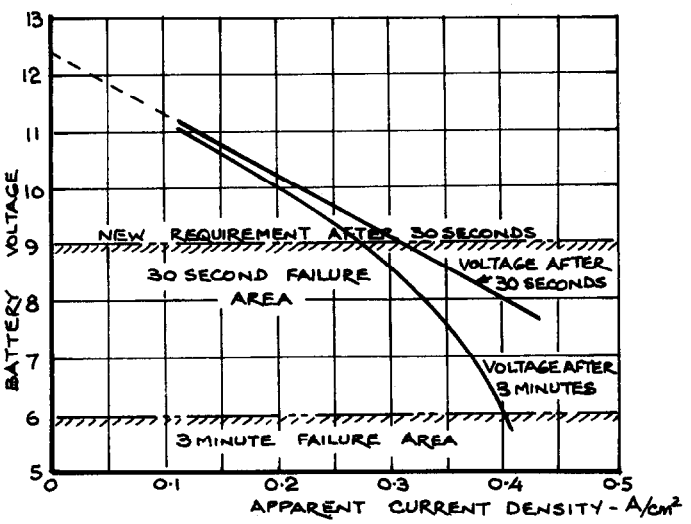

Fig. 9. Voltage vs. apparent current density characteristic for a 12-V, 40-Ah battery with the following design properties:

positive plates per cell	4
negative plates per cell	5
thickness of positive plate (mm)	1.9
thickness of negative plate (mm)	1.8
single surface area of active material per plate (cm^2)	126
overall thickness of separator (mm)	2.1
length of free electrolyte path (mm)	3.7
type of intercell connector	jumpover
plate pitch (mm)	8.3
temperature (°C)	−18

The original cold-start current of 180 A per cell of 4 positive and 5 negative plates is equivalent to an apparent density of $(180/4) \times 126 = 0.357$ A cm^{-2}, where the single surface area of the active material is 126 cm^2. At this apparent density, the average voltage after 30 s was 8.5 V, i.e., it just exceeded the minimum voltage required by specification. Assuming that the same thickness of plates and the same plate pitch was used in the redesigned battery, the average current density to give 9 V after 30 s will be 0.31 A cm^{-2}. This will require a plate area of: 210 A/0.31 A cm^{-2} = 677 cm^2 per cell. This requirement can be met by using more plates per cell of the same surface area as in the original battery, by using the same number of plates as in the original battery but of greater area, or by employing a combination of more plates of different size.

Taking the following design parameters for automotive plates:

• negative plates	
specific formed material weight	7.6 g (Ah)$^{-1}$
apparent formed density	3.4 g cm^{-3}
• positive plates	
specific formed material weight	8.8 g (Ah)$^{-1}$
apparent formed density	3.8 g cm^{-3}

The ratio of positive to negative material thickness would be about 1.04. This value is taken as a starting point for a redesign.

The same plate profile as in the original battery is used since it is unlikely that any significant increase can be accepted in the same container. Accordingly, each new cell would require 677/126 positive plates to give the required new current density. This gives 5.4 positive plates, i.e., 6 positive plates and 7 negative plates. The same compartment in the battery container that previously held 9 plates now has to accept 13 plates. This can only be achieved by reducing both the plate thickness and separator thickness.

A realistic minimum separator thickness is 1.25 mm. Accept this initially. Let t cm be the thickness of each negative plate and $1.04t$ cm that of the positive plate. Then:

$$6(1.04t) + 7t + (12 \times 1.25) + (6 \times 0.4) + 0.2 = 35 \text{ mm}$$

where the tolerance per pitch is assumed to be 0.4 mm and the tolerance per element 0.2 mm. This gives a negative thickness of 1.31 mm and a positive thickness of 1.37 cm. These values represent very thin plates that possibly will involve lower casting rates, higher scrap rates and operator retraining with, perhaps, newer and more sophisticated equipment. It is preferable, to avoid such drastic reductions in plate thicknesses. The alternatives are:

(i) to adopt a larger cell with 11 plates of an area of 135.5 cm^2 per plate;

(ii) to reduce the voltage losses in the separators, electrolyte path, pillars and connectors so that a standard profile can be used with two less plates;

(iii) to re-examine the paste formulation with the objective of increasing the active material porosity and reducing the true current density and the voltage polarization;

(iv) a combination of some or all of alternatives (i) to (iii).

Working on the basis of 11 plates per cell, each with an active material profile of 136 cm^2, examine the compartment dimensions to determine the tallest plate that can be accommodated sensibly without leading to electrolyte leakage. Within a container with an external width of 135 mm, the maximum plate width that can safely be used is of the order of 123 mm. Take a width of 120 mm, which on allowing 5 mm for the grid frame permits an active material width of 115 mm. The height of the plate

to provide 136 cm^2 active material area becomes $118+5=123$ mm. This should then be checked for acceptability within the cell compartment. If acceptable, calculate the approximate plate thicknesses as follows (note, take the positive plate as 1.04 times as thick as the negative and use the same tolerances and the same separator thickness as before):

$$5(1.04t)+6t+(10\times1.25)+(5\times0.4)+0.2=35 \text{ mm}$$

This gives a negative plate thickness of 1.81 mm and a positive of 1.88 mm.

These thicknesses are based on the use of a separator with a minimum thickness and could well introduce a capacity difficulty at a low rate through lack of sufficient electrolyte. Provided there is no reduction in the plate area (note, the attainment of the cold-start voltage depends on this), there is scope now with a relatively thick plate to make reductions. The extent of the reduction will be dictated by the volume of electrolyte that is available after adequate provision has been made for the volume of active materials capable of being reacted sufficiently to be supplied with electrolyte at the low rate. The redesigned battery is required to provide 45 Ah at the C_{20} rate. At this rate, it is realistic to react the electrolyte from 1.280 to 1.060 sp. gr. Referring to Fig. 16 in ref. 4, this will give a capacity potential for the electrolyte of 114 Ah l^{-1} or 8.8 cm^3 $(Ah)^{-1}$.

A realistic specific grid weight for a redesigned negative and positive is 5.5 and 7 g $(Ah)^{-1}$, respectively. These are not the lowest possible, but are fairly keen values and ensure that the design is not profligate in the use of metal. In ref. 4, recommended specific formed material weights of 7.6 and 8.8 g $(Ah)^{-1}$ for negative and positive material, respectively, were given for batteries subject to infrequent, deep discharging. These values are accepted initially.

It is envisaged that the electrolyte level will be just above the plate straps and the thickness of lugs will be the same as the relevant grid thickness. At the level of high-rate discharge currents expected, appropriate lug dimensions would be 10 mm wide and 8 mm above the top of the plates. Typical plate-strap dimensions would be 32 mm long by 15 mm wide by 5 mm thick. The electrolyte below the cell element is disregarded when estimating cell capacity.

A build-up of height dimensions from the bottom of a plate to the electrolyte level would be:

plate height (mm)	123
lug height (mm)	8
strap height (mm)	5
electrolyte over strap (mm)	5
total height (mm)	141

The capacity-producing electrolyte volume will be the internal volume of the cell compartment from the bottom of the plates to the electrolyte level, minus the volume of the solids within that space. The apparent volume of active materials will determine the plate material thickness.

apparent volume of negative material per cell (cm^3)	$\frac{7.6 \text{ g } (Ah)^{-1}\times45 \text{ Ah}}{3.4 \text{ g cm}^{-3}}=100.6$
apparent volume of negative material per plate (cm^3)	16.8
thickness of negative material (cm)	$\frac{16.8 \text{ cm}^3}{136 \text{ cm}^2}=0.125$

apparent volume of positive material per cell (cm^3)	$\frac{8.8\ g\ (Ah)^{-1} \times 45\ Ah}{3.8\ g\ cm^{-3}} = 104.2$
apparent volume of positive material per plate (cm^3)	20.8
positive material thickness (cm)	$\frac{20.8\ cm^3}{136\ cm^2} = 0.15$
volume of negative grids per cell (cm^3)	$\frac{5.5\ g\ (Ah)^{-1} \times 45\ Ah}{11.1\ g\ cm^{-3}} = 22.3$

It is assumed that the alloy is one with about 4.5 wt.% Sb

volume of positive grids per cell (cm^3)	$\frac{7\ g\ (Ah)^{-1} \times 45\ Ah}{11.1\ g\ cm^{-3}} = 28.4$
true volume of negative material per cell (cm^3)	$\frac{7.6\ g\ (Ah)^{-1} \times 45\ Ah}{11.3\ g\ cm^{-3}} = 30.3$
true volume of positive material per cell (cm^3)	$\frac{8.8\ g\ (Ah)^{-1} \times 45\ Ah}{9.4\ g\ cm^{-3}} = 42.1$
volume of lugs, negative (cm^3)	$6 \times 0.8 \times 1.0 \times 0.125 = 0.6$
volume of lugs, positive (cm^3)	$5 \times 0.8 \times 1.0 \times 0.15 = 0.6$
volume of plate straps (cm^3)	$2 \times 3.2 \times 1.5 \times 0.5 = 4.8$

The separators are as yet undefined and initially assumed to have a back web of 0.5 mm and an average thickness of 0.8 mm. This introduces an error if subsequently the overall thickness should differ from the value, but the order of error will not be large and will not alter significantly the ultimate results. The separators will overlap the plate width by about 2 mm on either side and thus make the separator width 124 mm. The separators will extend about 8 mm above the plate top so that they nest immediately below the plate straps. This makes the separator height 131 mm. Resin-impregnated paper separators are assumed with a volume porosity of about 50%.

volume of separators per cell (cm^3)	$10 \times 0.5 \times 13.1 \times 12.4 \times 0.08 = 65$
volume of cell compartment from bottom of plate to electrolyte level (cm^3)	$14.1 \times 13.0 \times 3.5 = 641.6$
volume of electrolyte (cm^3)	641.6 − volume of solids = 641.6 − 194.1 = 447.5
estimated capacity at 8.8 cm^3 $(Ah)^{-1}$ (Ah)	447.5/8.8 = 50.9, average

This is an acceptable result and should provide for all but the extremes of adverse tolerances.

If p mm is the new plate pitch and the internal width of a cell compartment is 35 mm, then:

$5p$ + negative plate thickness + 0.2 mm tolerance = 35 mm
$5p = 35 - (0.2 + 1.25)$
$p = 6.71$ mm, take 6.7 mm

This pitch will be made up of:

1 positive plate (mm)	1.5
1 negative plate (mm)	1.25
2 separators (mm)	3.6
pitch tolerance (mm)	0.35
total pitch (mm)	6.7

The cell arrangement to meet both the low-rate capacity and the cold-start performances will be one comprising 5 positive plates (120 mm (W) × 123 mm (H) × 1.5

mm (thick)), 6 negative plates (120 mm (W)×123 mm (H)×1.25 mm (thick)) with 10 separators (124 mm (W)×131 mm (H)×1.8 mm over ribs)). To achieve this, the plate pitch has been reduced from 8.3 to 6.7 mm, the separator thickness from 2.05 to 1.8 mm, the positive thickness from 1.9 to 1.5 mm, and the negative thickness from 1.8 to 1.25 mm. The effect of this is to reduce the voltage loss in the free electrolyte and to increase the loss in the grid and active materials.

Effect of reducing plate pitch and separator thickness

The free-electrolyte path has been reduced from 2.05 to 1.8 mm but the back-web thickness of the separators has remained at 0.5 mm, despite the reduction in the overall separator thickness. In the absence of definitive measurements of separator resistances, the retention of the same back-web thickness can be assumed to keep the separator resistance virtually constant.

The total surface area of the electrolyte path will change from (8×126) to (10×135) cm^2 and the specified cold-start current from 180 to 210 A.

resistance of original free-electrolyte path (Ω) $\frac{3.2\times0.205}{8\times126}=0.00065$

resistance of proposed new arrangement (Ω) $\frac{3.2\times0.180}{10\times135}=0.00043$

reduction in voltage loss per battery (V) $6(180\times0.00065-210\times0.00043)=0.16$

Effect of reducing the plate thicknesses

It is assumed that the same grid geometry is retained for the proposed new arrangement as for the original. The change in the grid and active material resistances will be close to direct proportionality with plate height and inversely proportional to the grid thickness. Although the parameters of the original standard battery have not been fully stated, and the individual voltage losses not calculated, the values for negative and positive plate resistances come out as (48.2×10^{-5}) and (55.04×10^{-5}) Ω, respectively.

The equivalent resistances for the proposed design then become:

- negative plate

thickness is changed from 1.8 to 1.25 mm
height is changed from 114 to 122 mm
estimated resistance of new plate (Ω) $=48.2\times10^{-5}\times(122/114)\times(1.8/1.25)=74.3\times10^{-5}$

- positive plate

thickness is changed from 1.9 to 1.5 mm
height is changed from 114 to 122 mm
estimated resistance of new plate (Ω) $=55.4\times10^{-5}\times(122/114)\times(1.9/1.5)=75.1\times10^{-5}$
voltage loss in original plate (V) $=(180/4)\times(48.2\times10^{-5}+55.04\times10^{-5})=0.046$
voltage loss in proposed plate (V) $=(210/5)\times(74.3\times10^{-5}+75.1\times10^{-5})=0.063$
increased voltage loss per battery (V) $=6(0.063-0.046)=0.1$

The nett effect of the changes in plates and separation is a small improvement in the cold-start voltage of the order of 0.06 V. This is almost negligible and, although there should not be any trouble in meeting the full low-rate capacity when all the tolerances act adversely, the same cannot be said for the cold-start performances. It

is generally experienced, however, that the full play of tolerances do not alter the cold-start voltages as much as they alter the low-rate capacities. If possible, a further easement in the voltage losses by other design changes would remove the reliance of the cold-start performance on tight quality control of the materials and processing. The tighter the quality control in production, the more costly, in general, is the product and the aim of a good design is to allow the adoption of relatively easy tolerances. If the cold-start performance could have been achieved without any effort in design, then the selection of comfortable tolerances becomes easy. This is not, however, the case in the example just considered. The introduction of other easements to improve the voltage loss would be welcomed.

The connector used in the design was of the 'jump-over'-type as in the standard battery and the possibility of adopting the shorter 'through-the-wall'-type should be explored by seeking the supply of equivalent dimensioned containers designed to accept the latter connector. If this can be achieved, the change in connector design should be adopted to increase the safety margin and ease the production tolerances.

Referring to Fig. 9, whilst the attainment of the cold-start voltage after 30 s may mean a relatively tight quality control, there is ample margin in the 3-min requirement of not less than 6 V.

If, in the foregoing exercise, it was found that the increased height of plate and improvement in connector design could not be accommodated in the available containers of the dimensions specified, then there is no alternative to a careful series of planned experiments to optimize both the organic expander content, the porosities of the active materials, and the developed internal surface areas within the active materials. The latter is a function of the particle-size distribution of the oxide, the porosity of the formed material, and the amount of material from which the plates are made.

References

1 L. Prout, *J. Power Sources, 41* (1992) 107.
2 J.T. Crennell and F.M. Lea, *J. Inst. Elect. Eng., 66* (1928) 529.
3 U.B. Thomas, *J. Electrochem. Soc., 94* (1948) 42.
4 L. Prout, *J. Power Sources, 46* (1993) 73.